Remote Sensing of Environment 151 (2014) 166–174

Contents lists available at ScienceDirect

Remote Sensing of Environment

journal homepage: www.elsevier.com/locate/rse

Airborne laser scanner-assisted estimation of aboveground biomass change in a temperate oak–pine forest

Nicholas S. Skowronski [a,*], Kenneth L. Clark [b], Michael Gallagher [b], Richard A. Birdsey [c], John L. Hom [c]

[a] USDA Forest Service, Northern Research Station, Morgantown, WV 26505, USA
[b] USDA Forest Service, Northern Research Station, New Lisbon, NJ 08064, USA
[c] USDA Forest Service, Northern Research Station, Newtown Square, PA 19073, USA

ARTICLE INFO

Article history:
Received 25 November 2012
Received in revised form 10 December 2013
Accepted 12 December 2013
Available online 16 January 2014

Keywords:
Airborne laser scanning
ALS
Disturbance
Multi-temporal
Biomass change estimation
New Jersey Pinelands

ABSTRACT

We estimated aboveground tree biomass and change in aboveground tree biomass using repeated airborne laser scanner (ALS) acquisitions and temporally coincident ground observations of forest biomass, for a relatively undisturbed period (2004–2007; Δ_{07-04}), a contrasting period of disturbance (2007–2009; Δ_{09-07}), and an integrated period (2004–2009; Δ_{09-04}). A simple random sampling (SRS) estimator was used to estimate means and variances of biomass and biomass change for each measurement occasion and interval. For each year, linear regression models were used to predict mean total aboveground tree biomass for live, dead, and total biomass components from ALS-derived variables. These models predicted biomass with $R^2 = 0.68$, 0.59, and 0.70 and RMSEs of 32.7, 30.5, and 31.7 Mg ha^{-1} for 2004, 2007 and 2009, respectively. A model assisted indirect estimator was then used to estimate biomass and biomass change for comparison to the field-based SRS estimator. This model assisted indirect approach decreased standard errors of biomass estimation relative to the SRS estimator, but had larger variances for biomass change estimation. Linear regression models were also used to directly predict field-estimated biomass change using ALS Δ-variables, calculated as the difference between multi-temporal ALS variables, for the study area. Integrated over the 6 year period, these change models had $R^2 = 0.81$, 0.72, and 0.68 with RMSEs of 2.0, 9.3, and 1.0 Mg ha^{-1} yr^{-1} for live, dead, and total aboveground tree biomass, respectively. A model assisted direct estimator reduced standard errors of change estimates by 100–200% compared to the field-based estimates. We discuss several potential advantages and limitations of the direct and indirect approaches. Our primary finding is that model assisted direct estimation of biomass change decreased estimation uncertainty relative to both field and model assisted indirect estimation.

Published by Elsevier Inc.

1. Introduction

There is large uncertainty in the carbon sink strength of terrestrial ecosystems, recently estimated at 1.1 ± 0.8 Pg C yr^{-1} globally (Pan et al., 2011). In response, several international initiatives are aimed at increasing the precision of forest biomass and estimates of biomass change at multiple spatial and temporal scales. These include, but are not limited to, the United Nations Collaborative Programme on Reducing Emissions from Deforestation and Forest Degradation in Developing Countries (UN-REDD; http://www.un-redd.org), the Kyoto Protocol's Land Use, Land Use Change and Forestry section (IPCC, 2006) and the North American Carbon Program (NACP; http://www.nacarbon.org/nacp). These initiatives have brought into focus the need for repeatable, cost-effective, and simple remote sensing methodologies for monitoring, reporting, and verification (MRV) of biomass stocks (Goetz & Dubayah, 2011).

The estimation of change in biomass stocks is an area of particular interest (Houghton, Hall, & Goetz, 2009). Because of strong interest in the net exchange of CO_2 between the land and the atmosphere, it may be more important that we understand the trajectory of the global carbon storage than to accurately estimate the storage itself. The estimation of biomass loss and accumulation through time as a response to various disturbance events presents methodological challenges, particularly at larger spatial scales (Goetz et al., 2012). Disturbances such as wildfire, hurricanes, and insect invasions impact both standing biomass and the future rates of change in these pools. Spatially, we have been able to incorporate time-series spatial reflectance data to illustrate the extent and patterning of disturbance at high temporal resolution (e.g., Zhu, Woodcock, & Olofsson, 2012) and broad spatial scales (e.g., Blackard et al., 2008; Masek et al., 2008). Many studies have demonstrated, under some conditions, the ability of spatial reflectance data to reflect the severity of disturbance, particularly in the realm of wildland fire intensity (e.g., Keeley, 2009; Veraverbeke & Hook, 2013).

The application of Light Detection and Ranging (LiDAR) data to the problem of mapping and estimation of terrestrial biomass has been shown to greatly increase the spatial resolution and accuracy of aboveground biomass estimates in many studies (see Asner et al., 2010, 2011;

* Corresponding author at: 180 Canfield Street, Morgantown, WV 26505, USA. Tel.: +1 304 285 1507.
E-mail address: nskowronski@fs.fed.us (N.S. Skowronski).

0034-4257/$ – see front matter. Published by Elsevier Inc.
http://dx.doi.org/10.1016/j.rse.2013.12.015

Zolkos, Goetz, & Dubayah, 2013). Several recent studies have incorporated more thorough statistical techniques to estimate the uncertainty of various biomass estimators across landscapes (Mascaro, Detto, Asner, & Muller-Landau, 2011; Næsset et al. 2011), with one example reporting uncertainty at <1% (standard error of the mean; SE) of the estimated landscape-scale mean carbon density (Gonzalez et al., 2010). Several studies have successfully decreased estimation uncertainty while maximizing cost-effectiveness by targeting airborne laser scanner (ALS) data collections to sample small portions of the population, rather than gathering wall to wall data (e.g., Andersen, Strunk, Temesgen, Atwood, & Winterberger, 2012, Gobakken et al., 2012). This work has been complemented by additional simulation studies that were designed to optimize sampling designs in ways that maximized sampling efficiency while minimizing estimation uncertainty (Ene et al., 2012, 2013).

The characterization of change using multi-date ALS acquisitions has not received the same attention as single-date characterization because of the overall paucity of these repeated-measure datasets. However, as multi-temporal datasets have become available, several studies have demonstrated the utility of this approach. For example, Solberg, Næsset, Hanssen, and Christiansen (2006) illustrated the use of repeated ALS acquisitions to detect changes in LAI during an insect attack on Scots pine (*Pinus sylvestris* L.) in Norway. Additional research has documented canopy gap formation and closure over two time periods (Vepakomma, St-Onge, & Keenshaw, 2008, 2011). The estimation of individual stem height growth has also been reported in several studies (Yu, Hyyppä, Kaartinen, & Maltamo, 2004; Yu et al., 2005; Yu, Hyyppä, Kukko, Maltamo, & Kaartinen, 2006). Additionally, Næsset and Gobakken (2005), Hopkinson, Chasmer, and Hall (2008), and Yu, Hyyppä, Kaartinen, Maltamo, and Hyyppä (2008) reported that they were able to estimate mean height and volume change at the plot level, albeit with low precision.

Even fewer studies have addressed the efficacy of using multi-date LiDAR acquisitions for the estimation of biomass change. Dubayah et al. (2010) used large-footprint airborne LiDAR data (LVIS) to estimate forest structure and biomass change at 1 ha resolution at La Selva Biological Station, Costa Rica. They reported success at estimating change in younger forest areas, but were not able to discern increment in older stands. Hudak et al. (2012) employed multi-date ALS acquisitions to estimate biomass changes in an actively-managed forest landscape and concluded that their methodology of modeling biomass separately for two ALS acquisitions and differencing the resultant model outputs yielded estimates of biomass change that could be used to monitor biomass change and carbon flux across large tracts of land. Both Næsset, Bollandsås, Gobakken, Gregoire, and Ståhl (2013) and Bollandsås, Gregoire, Næsset, and Øyen (2013) employed a similar indirect estimation technique as Hudak et al. (2012), and also directly modeled the change in biomass using corresponding change in predictor variables (Δ-variables) derived from the ALS datasets. Bollandsås et al. (2013) indicated that this direct prediction methodology produced smaller residuals and RMSEs than the indirect approach. Næsset et al. (2013) also indicated a smaller standard error of the landscape mean biomass change using a similar direct modeling and estimation approach.

The potential for using ALS as an auxiliary dataset for improving estimates of forest attribute change is exciting in many fields. Of particular interest is the estimation of changes to these attributes following disturbance events such as wildfire, insect defoliation, or blowdown events. Linking spatially explicit estimates of attribute change with stratification schemes would allow for categorical assessment of these events, thereby increasing reporting precision and contributing to the analysis of events that may be spatially complex and thus difficult to capture with traditional field inventories. However, the paucity of repeated ALS datasets and the scarcity of appropriately re-measured inventory data within their bounds have limited the study and application of ALS-based change estimation. Thus, fundamental studies are necessary to develop a knowledge base that builds towards estimating complex biomass changes with improved estimation uncertainties.

Our study aims to estimate aboveground biomass change for disturbed and undisturbed time periods using multitemporal ALS datasets. Specifically, our objective was to compare the effectiveness of model-assisted direct and indirect approaches for estimating biomass and biomass change over a 3 × 3 km area using three repeated ALS datasets as auxiliary data. The repeated ALS acquisitions allowed us to compare estimates developed over two contrasting time periods. The first time period (3 years) had little field observed mortality while the second period (2 years) included extensive, heterogeneous, stem mortality following Gypsy moth (*Lymantria dispar*) defoliation. We also integrated both time periods for a 5-year analysis of biomass change. We explored three techniques for the estimation of biomass change. As the first method, we used a field-based simple random sampling estimator of aboveground biomass change. We then used linear regression models to predict biomass across the study area for each of the three ALS acquisitions. The second method indirectly estimated mean biomass change by differencing estimates of biomass for two measurement occasions. The third method used models to directly predict the change in biomass over three time periods in response to corresponding changes in ALS predictor variables. These predictions were then used to directly estimate mean biomass change across the study area. While primarily focused on comparing approaches for change estimation, this work also provides analysis that informs several other knowledge gaps. For instance, there is no literature currently available that demonstrates and evaluates the efficacy of using repeated ALS datasets to estimate biomass change on the Atlantic Coastal Plain of the United States. Additionally, there are few studies that provide estimates of biomass change before and after heterogeneous, non-stand replacing disturbance events.

2. Data

The study site is located in Burlington County, New Jersey, USA, within the Pinelands Management Area (PMA), a UNESCO MAB reserve site (Fig. 1; Latitude 39° 54′ 58.70″ N, Longitude 74° 35′ 51.38″ W). The study area is 3 × 3 km centered on an eddy-covariance and meteorological tower at the Silas Little Experimental Forest (SLEF) in New Lisbon, NJ (Fig. 1). The vegetation within the spatial extent of the site is composed of a predominantly oak (*Quercus* spp.) overstory with some pitch (*Pinus rigida* L.) and shortleaf pines (*Pinus echinata* Mill.). The understory is dense, and consists mostly of oak and pine saplings, scrub oaks, and shrubs, primarily huckleberry (*Gaylussacia* spp.) and blueberry (*Vaccinium* spp.). Much of the study area experienced defoliation by Gypsy moth over three years, beginning in 2006. The intensity of this disturbance was uneven and caused a spatially variable amount of stem mortality of mature oaks through the course of the study (see Clark, Skowronski, Gallagher, Renninger, & Schäfer, 2012; Clark, Skowronski, & Hom, 2010).

2.1. Field data

We installed 16 forest survey plots, patterned after the United States Department of Agriculture, Forest Service, Forest Inventory and Analysis (FIA) plot protocol (http://www.fia.fs.fed.us/), in a regular 4 by 4 pattern following the NACP Tier 3 plot design (Fig. 1; Hollinger, 2008). Each plot consisted of four circular 14.6 m diameter subplots (0.07 ha), with one subplot located in the center and three equidistant subplots distributed symmetrically around and located 36.6 m from the center subplot. 63 sub-plots were available for analysis following the rejection of a plot that was partially located on a non-forested area. Subplot centers were spatially recorded using a differentially corrected GPS (Pathfinder ProXT, Model # 52240-20, Trimble Navigation Limited, Sunnydale, CA). We made use of variables from the 63 subplots, as opposed to the 16 aggregated plots, to increase the number of data points available for biomass and biomass change predictive model fitting. This design is somewhat problematic because of the potential for spatial correlation between observations, given their

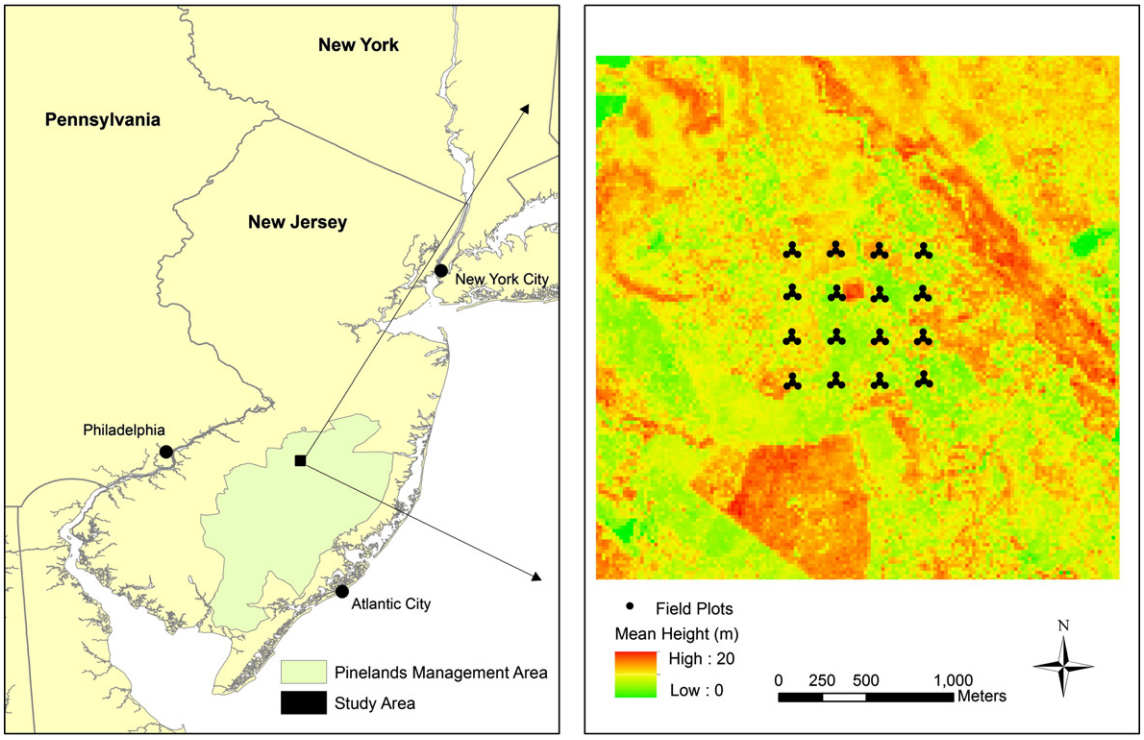

Fig. 1. Location of the study area. The right panel illustrates the study area extent and spatial arrangement of field plots overlaid on the mean canopy height from the 2007 ALS dataset.

clustered arrangement. We addressed this issue by testing for spatial correlation of model residuals, described in further detail below.

Plots were measured during the dormant season, December through February, of 2004, 2007, and 2009 (T_{04}, T_{07}, and T_{09}). The initial, T_{04}, measurement occurred before any evidence of gypsy moth defoliation, which was first observed in 2006 (Clark et al., 2010). Trees greater than 12.7 cm in diameter (at 1.37 m height from the forest floor, dbh) were measured for species, dbh, canopy base-height, height and status (live/dead) in each plot at each time step. Live and dead stem density (D_{live} and D_{dead}, respectively; stems ha^{-1}) and live and dead basal area (BA_{live} and BA_{dead}, respectively; m^2 ha^{-1}) were estimated for every plot at each time step. We used allometric models from various sources (Clark, Phillips, & Frederick, 1985, 1986; Hocker & Early, 1983; Jenkins, Chojnacky, Heath, & Birdsey, 2004; Martin, Kloeppel, Schaefer, Kimbler, & McNulty, 1998; Perala & Alban, 1994; Whittaker & Woodwell, 1968; Young, Ribe, & Wainwright, 1980) to estimate live, dead and total tree biomass (B_{live}, B_{dead}, and B_{total}, respectively; Mg ha^{-1}). We estimated the mean annual change of each variable for the three measurement periods: 2004–2007 (Δ_{07-04}), 2007–2009 (Δ_{09-07}), and 2004–2009 (Δ_{09-04}). The observations of the response variables were then averaged over the measurement period to represent a single year time-step (e.g., Mg ha^{-1} yr^{-1}) to maintain comparability as the periods differed in length.

2.2. ALS data

ALS data were acquired three times over the course of the study. These data were collected during times of maximum leaf-area in the growing season prior to each field data collection (October 2004, June 2006, and October 2008). To maintain consistency with the corresponding field dataset, we refer to these acquisitions by their corresponding field measured year (T_{04_ALS}, T_{07_ALS}, and T_{09_ALS}, respectively). The T_{04_ALS} and T_{07_ALS} datasets were collected with an Optech ALTM 2050 with average densities of 1.6 and 5.9 pulses m^{-2}, respectively. The T_{09_ALS} dataset was collected with a Leica ALS60 with an average density of approximately 4.8 pulses m^{-2}.

We used the Toolbox for LiDAR Data Filtering and Forest Studies (TiFFS; Chen, 2007) to estimate digital elevation models (DEMs), canopy height models (CHMs), and statistical predictor variables for each acquisition. The three ALS datasets were processed using a consistent spatial origin to ensure a uniform spatial extent and geographic consistency between their respective gridded data products. DEMs were estimated using all available returns at 1×1 m resolution by the TiFFS filtering algorithm (Chen, 2007). Return height values were then adjusted to represent their height above corresponding DEM grid cells. We estimated ALS predictor variables within the spatial extent of each sub-plot for model fitting. These same predictor variables were also estimated for a lattice of 25×25 m cells that covered the 3×3 km study area. Only first returns at least 1 m above the estimated ground level were used for the estimation of predictor variables. Predictor variables included percent cover (non-ground returns/all returns), percent cover at height greater than 4 m, mean height, maximum return height, standard deviation, skewness, kurtosis, and decile heights ($p10$–$p90$) (see Næsset, 2002). Additionally, a canopy height profile was estimated, accounting for optical occlusion per MacArthur and Horn (1969), and these predictor variables were estimated for discrete 1 m height bins (1–2 m, 2–3 m…24–25 m), the sum of the canopy height profile, and the maximum of the profile for each cell, following Skowronski, Clark, Duveneck, and Hom (2011). Additionally, similar to the approach taken by Bollandsås et al. (2013), we estimated Δ-variables that were the difference of each ALS variable between corresponding ALS acquisitions. For example, the difference between 2009 $p10$ and 2007 $p10$ is represented as $p10_{\Delta 09-07}$. These Δ-variables were estimated for Δ_{07-04}, Δ_{09-07}, and Δ09–04 (e.g., $p10_{\Delta 09-07}$, $p10_{\Delta 09-07}$, and $p10_{\Delta 09-04}$).

3. Methods

3.1. Biomass and biomass change models

We first developed models to predict biomass for each measurement occasion. We fit OLS linear regression models for all-subsets and ranked

the models by their respective adjusted coefficient of determination (adj. R^2), to predict B_{live}, B_{dead}, and B_{total} from the individual ALS variable sets for 2004, 2007 and 2009. We used adj. R^2 as our ranking statistic because it adjusts to the number of parameters used in a model and increases only when a new term improves the model, as opposed to the coefficient of determination (R^2) which increases with the addition of a new term regardless of model improvement. We then selected the model that used the fewest predictor variables from the 10 highest ranked models for each biomass component and measurement occasion. As a form of cross validation, we calculated the predicted residual sum of squares (PRESS) statistic (Myers, 1990) for each selected model. PRESS is calculated by iteratively omitting a single observation from the estimation of a model and then computing the sum of the squared residuals. The root mean square error (RMSE) of the PRESS statistic was then compared to the RMSE of the full model to characterize model overparameterization. We confirmed that residual variance was homoscedastic in each model using White's test (White, 1980). The clustered nature of the sampling scheme caused concern over spatial correlation of the sample data so we also calculated an omni-directional Moran's I coefficient to test the residuals of each model for spatial correlation. These calculations were made with a lag of 50 m to ensure the calculation related each of the 4 sub-plots in a single FIA plot. Biomass change was then estimated by differencing study area-wide estimates of mean biomass for each time period.

We then directly predicted the change in biomass as a response to the change in ALS-derived Δ-variables for each cell over the two time steps. We first calculated the changes in the aboveground biomass pools of the field-measured plots for the three measurement periods. We then fit OLS linear regression models for all-subsets and ranked the models by their respective adjusted coefficient of determination (adj. R^2), to predict the changes in B_{live}, B_{dead}, and B_{total} for the measurement intervals (Δ_{07-04}, Δ_{09-07}, and Δ_{all}). We again used adj. R^2 as our ranking statistic and selected the model that used the fewest predictor variables from the 10 highest ranked models for each biomass component and time step. For cross validation, we again compared the RMSE of the PRESS statistic to the RMSE of the full model. As above, we confirmed that residual variance of these change models was homoscedastic using White's test. Residuals were tested for spatial correlation using an omni-directional Moran's I coefficient at a lag of 50 m.

3.2. Estimators

Here, we provide estimates of mean biomass and biomass change and associated variances from the three approaches: field-based simple random sampling estimation, model-assisted indirect estimation, and model assisted direct estimation. Calculating the ratios of the variances, or relative efficiencies (REs), of various approaches allows us to evaluate the added benefit of combining auxiliary ALS data with a field survey and to compare the results obtained between the direct and indirect modeling approaches.

3.2.1. Simple random sampling estimation

We estimated population means of biomass and biomass change from field sample data using the simple random sample (SRS) estimator given in McRoberts, Næsset, and Gobakken (2013). In this case, FIA subplot data was aggregated to represent a single FIA-type plot ($n = 16$). This is consistent with the approach that is taken by the FIA program. We let y represent the observed biomass (b) or biomass change (Δb) for the field observations (n), and let μ denote the mean biomass (B) per unit area or mean biomass change per unit area (ΔB) for sampling year or interval (t; T_{04}, T_{07}, and T_{09}; Δ_{07-04}, Δ_{09-07}, and Δ_{all}) and for components (c; B_{live}, B_{dead}, and B_{total}; ΔB_{live}, ΔB_{dead}, and ΔB_{total}). We then estimated the mean for each set as:

$$\hat{\mu}_{SRStc} = \frac{1}{n}\sum_{k\in tc} y_k, \tag{1}$$

where k indexes the n sample observations and y_k is the observation for the kth population unit selected from the sample. A variance estimator is given as:

$$\hat{Var}_{SRStc}(\hat{\mu}_{SRStc}) = \frac{\sum_{k\in tc}(y_k - \hat{\mu}_{SRS})^2}{n(n-1)}. \tag{2}$$

While the variance estimator $\hat{Var}_{tc}(\hat{\mu}_{SRStc})$ is likely biased because of our systematic sampling design, this bias is likely to result in an overestimate of the true variance (McRoberts et al., 2013; Næsset et al., 2013; Särndal et al., 1992, p. 83).

3.2.2. Model-assisted estimation

Model-assisted estimation uses models and auxiliary variables, in our case ALS-derived, to produce areal estimates of parameters and estimation uncertainties at various scales. We utilized the ALS variables to predict biomass and biomass change for every population element and to assist in the estimation of corresponding means over the entire study area. Here, because the predictive models were developed using the subplots, rather than the aggregated plots, we estimated variances using all subplots ($n = 63$). We used the regression models constructed in Section 3.1 to predict $\hat{y}$ for t and c using the direct and indirect models developed with the ALS auxiliary dataset above for the samples n. In this case, we let N denote the population size of 25 × 25 m grid cells for the study area and we assume the availability of the auxiliary ALS data for each grid cell. Further, we let m denote the modeling approach used for estimating û, either the direct or indirect approach. We then used the model-assisted (MA) estimator presented by McRoberts (2010) that was based on Särndal et al. (1992, pp. 221–225) as:

$$\hat{\mu}^m_{MAtc} = \frac{1}{N}\sum_{k\in tc}\hat{y}^m_k - \frac{1}{n}\sum_{i\in tc}(\hat{y}^m_k - y_k), \tag{3}$$

where $\hat{y}_k$ is predicted for every population element from the modeling described above and $\frac{1}{n}\sum_{k\in tc}(\hat{y}^m_k - y_k)$ is an estimator of the bias. The variance for the direct (d) modeling approach is given as,

$$\hat{Var}^d_{MAtc}\left(\hat{\mu}^d_{MAtc}\right) = \frac{1}{n(n-1)}\sum_{k\in tc}\left(\varepsilon^d_k - \bar{\varepsilon}^d_k\right)^2, \tag{4}$$

where $\varepsilon^d_k = \hat{y}^d_k - y_k$ and $\bar{\varepsilon}^d_k$ is the mean of the errors. The variance for the indirect method (i) is estimated as,

$$\begin{aligned}\hat{Var}^i_{MAtc}\left(\Delta\hat{\mu}^i_{MAtc}\right) &= \hat{Var}^i_{MAtc}\left(\hat{\mu}^2_{MAtc} - \hat{\mu}^1_{MAtc}\right)\\ &= \hat{Var}^i_{MAtc}\left(\hat{\mu}^1_{MAtc}\right) - 2\hat{Cov}\left(\hat{\mu}^2_{MAtc}, \hat{\mu}^1_{MAtc}\right) + \hat{Var}^i_{MAtc}\left(\hat{\mu}^2_{MAtc}\right),\end{aligned} \tag{5}$$

where the superscripts denote times 1 and 2. Because the temporal predictions are from the same mapping units, the covariance is estimated as,

$$\hat{Cov}\left(\hat{\mu}^2_{MAtc}, \hat{\mu}^1_{MAtc}\right) = \frac{1}{n(n-1)}\sum_{k\in tc}\left(\delta^1_k - \bar{\delta}^1\right)\left(\delta^2_k - \bar{\delta}^2\right), \tag{6}$$

where $\delta^1_k = \hat{y}^1_k - y^1_k$ and $\delta^2_k = \hat{y}^2_k - y^2_k$ are errors and $\bar{\delta}^1$ and $\bar{\delta}^2$ are the means of these errors, again for times 1 and 2. Thus, we were able to develop estimates of biomass and their associated variances for the field-based and direct and indirect modeling approaches. We use relative efficiency (RE) as a way to compare the precision of the two contrasting modeling approaches for the study area, given as:

$$RE = \frac{\hat{Var}_{SRStc}(\hat{\mu}_{SRStc})}{\hat{Var}^m_{MAtc}(\hat{\mu}^m_{MAtc})}. \tag{7}$$

This ratio allows for the evaluation of the two model-assisted estimators, with instances greater than 1.0 indicating an improvement over the variance as they relate to the field-based estimate.

4. Results

4.1. Field-based SRS estimators and estimation

We estimated biomass for the study area using SRS for estimation from the field survey data. The field-based estimates of total aboveground biomass were 83.7 (SE = 5.0) in 2004, 88.1 (SE = 5.0) in 2007, and 93.1 (SE = 4.9) Mg ha^{-1} in 2009 (Table 1). Estimates of live tree biomass from the field survey were similar in magnitude to total tree biomass at 82.4 (SE = 4.5), 87.6 (SE = 4.6) and 83.4 (SE = 4.5) Mg ha^{-1} for 2004, 2007, and 2009, respectively (Table 1). Live tree biomass increased between 2004 and 2007 because of stem increment, and decreased between 2007 and 2009 because of mortality resulting from defoliation by Gypsy moth in 2007 and 2008.

The field-based SRS estimates of biomass change illustrate a contrast between the Δ_{07-04} and Δ_{09-07} measurement periods. For Δ_{07-04}, field estimated B_{live} increased at a mean rate of 1.7 (SE = 0.2) Mg ha^{-1} yr^{-1} while the B_{dead} pool decreased at a rate of −0.1 (SE = 0.1; Table 1) Mg ha^{-1} yr^{-1}. Conversely, for Δ_{09-07}, the estimated B_{live} pool decreased at a rate of −2.0 Mg ha^{-1} yr^{-1} (SE = 1.7) while the dead pool increased at a rate of 4.6 Mg ha^{-1} yr^{-1} (SE = 1.4 Mg ha^{-1}; Table 1). However, somewhat counter intuitively, mean B_{total} change is greater for Δ_{09-07} than Δ_{07-04}, 2.5 and 1.5 Mg ha^{-1} yr^{-1} (SE = 0.6 and 0.2 Mg ha^{-1} yr^{-1}), respectively, even with the increased stem mortality (Table 1). When integrated over the entire time period (Δ_{09-04}), biomass change was estimated as 0.2 Mg ha^{-1} yr^{-1} (SE = 0.6 Mg ha^{-1} yr^{-1}), 1.7 Mg ha^{-1} yr^{-1} (SE = 0.5 Mg ha^{-1} yr^{-1}) and 1.9 Mg ha^{-1} yr^{-1} (SE = 0.3 Mg ha^{-1} yr^{-1}) for the live, dead, and total pools, respectively.

4.2. Model-assisted indirect estimator

4.2.1. Models

The statistical characteristics of the models selected to predict biomass using the auxiliary ALS data are presented in Table 2. The spatial correlation of residuals was not found to be statistically significantly different from zero (Moran's I, $p > 0.05$). The selected models were relatively consistent in strength for all three measurement occasions (T_{04}, T_{07}, and T_{09}). Coefficients of determination ranged from 0.59 to 0.69 and 0.59–0.70 for live tree biomass and total tree biomass estimation, respectively (Table 2). Fig. 2A–C presents the relationships between observed and predicted values of B_{total} for T_{04}, T_{07}, and T_{09}l. For B_{dead}, the coefficients of determination are statistically significant, but weaker than the B_{live} and B_{total} models for T_{04}, T_{07}, and T_{09} ($0.41 \leq R^2 \leq 0.47$, Table 2). The RMSEs relative to the means (73%–196%, Table 2) indicate poor model fit for B_{dead}. The $RMSE_{PRESS}$ statistics for all models of B_{live}, B_{dead}, and B_{total} illustrate a consistent overfit, which can be attributed to the relatively low variability within, and poor correlation of the ALS predictor variables to, the field-based estimates. Lack of fit is evident in these models (Fig. 2A–C) as there is systematic over-prediction of small biomass values and under-prediction of larger values.

Table 2
Statistics of aboveground biomass models for 2004, 2007, and 2009 (n = 63).

	$n(v)$	$RMSE_{reg}$	$RMSE_{PRESS}$	R^2	Adj. R^2
Live tree biomass (B_{live})					
T_{04}	17	23.6 (29%)	32.7 (40%)	0.69	0.57
T_{07}	10	25.6 (29%)	30.5 (34%)	0.59	0.51
T_{09}	16	23.1 (28%)	31.7 (38%)	0.69	0.57
Dead tree biomass (B_{dead})					
T_{04}	18	2.3 (196%)	3.7 (313%)	0.42	0.18
T_{07}	16	1.7 (225%)	2.9 (476%)	0.47	0.28
T_{09}	11	13.6 (137%)	17.2 (174%)	0.43	0.30
Total tree biomass (B_{total})					
T_{04}	16	23.7 (28%)	30.9 (37%)	0.68	0.56
T_{07}	10	23.3 (29%)	30.3 (34%)	0.59	0.51
T_{09}	18	23.8 (26%)	32.2 (34%)	0.70	0.58

$n(v)$ = number of predictor variables used in the model, $RMSE_{reg}$ = root mean square error of the regression (Mg ha^{-1}, % of mean), $RMSE_{PRESS}$ = root mean square error of the PRESS statistic (Mg ha^{-1}, % of mean), R^2 = coefficient of determination, Adj. R^2 = adjusted R^2.

4.2.2. Estimation

The model-assisted indirect estimates of total tree biomass were 110.1 (SE = 2.6) for 2004, 106.4 (SE = 3.0) for 2007, and 95.8 (SE = 2.5) Mg ha^{-1} for 2009 (Table 1). The use of the model assisted indirect estimation produced REs ranging from 2.8 to 3.8 for total tree biomass over the 3 surveys. Model assisted indirect estimates of live tree biomass ranged from 74.7 to 91.9 Mg ha^{-1} and from 2.2 to 2.6 for standard errors (Table 1). RE for live tree biomass ranged from 2.9 to 5.0. Model-assisted indirect estimates of dead tree biomass and standard errors were similar to field estimates (Table 1) and produced REs ranging from 0.8 to 6.3.

For biomass change, the model-assisted indirect approach yielded estimates of the total change in biomass of −1.2 (SE = 1.4), −5.3 (SE = 1.6), and −2.9 (SE = 1.6) Mg ha^{-1} yr^{-1}, for Δ_{07-04}, Δ_{09-07}, and Δ_{09-04}, respectively (Table 1). Live biomass change was estimated as 4.7 (SE = 1.5), 0.7 (SE = 1.6), and 3.4 (SE = 1.6) Mg ha^{-1} yr^{-1} for the same periods, respectively (Table 1). For the majority of biomass change components and measurement intervals, indirect estimation yielded fractional REs (0.01–0.18). Only the estimation of the biomass change in the live (RE = 1.1) and dead (RE = 1.3) components in Δ_{09-07} yielded improved efficiency over the field-based SRS estimators.

4.3. Model-assisted direct estimator

4.3.1. Models

For the Δ_{07-04} period, the direct estimation approach produced models that explained a statistically significant portion of the

Table 1
Estimated mean biomass and biomass change and associated standard error (SE) of the estimates.

	Field estimate						Model-assisted direct estimate						Model-assisted indirect estimate					
	Live		Dead		Total		Live		Dead		Total		Live		Dead		Total	
	Mean	SE	Mean	SE	Mean	SE	Mean	SE	Mean	SE	Mean	SE	Mean	SE	Mean	SE	Mean	SE
Biomass (Mg ha^{-1})																		
T_{04}	82.4	4.9	1.2	0.5	83.7	5.0	[a]	[a]	[a]	[a]	[a]	[a]	74.7	2.2	2.2	0.2	110.1	2.6
T_{07}	87.4	5.1	0.8	0.2	88.1	5.0	[a]	[a]	[a]	[a]	[a]	[a]	88.9	2.8	2.1	0.2	106.4	3.0
T_{09}	83.3	4.4	9.8	2.9	93.1	4.9	[a]	[a]	[a]	[a]	[a]	[a]	91.9	2.6	6.6	1.5	95.8	2.5
Biomass Δ (Mg ha^{-1} yr^{-1})																		
Δ_{07-04}	1.7	0.2	−0.1	0.1	1.5	0.2	2.3	0.1	−0.3	0.1	2.9	0.1	4.7	1.5	−0.1	0.5	−1.2	1.4
Δ_{09-07}	−2.0	1.7	4.6	1.4	2.5	0.6	0.6	0.7	0.7	0.7	1.6	0.3	0.7	1.6	1.1	1.3	−5.3	1.6
Δ_{09-04}	0.2	0.6	1.7	0.5	1.9	0.3	1.8	0.2	0.5	0.2	2.5	0.1	3.4	1.6	0.9	1.3	−2.9	1.6

[a] Biomass was not estimated in the direct estimation methodology.

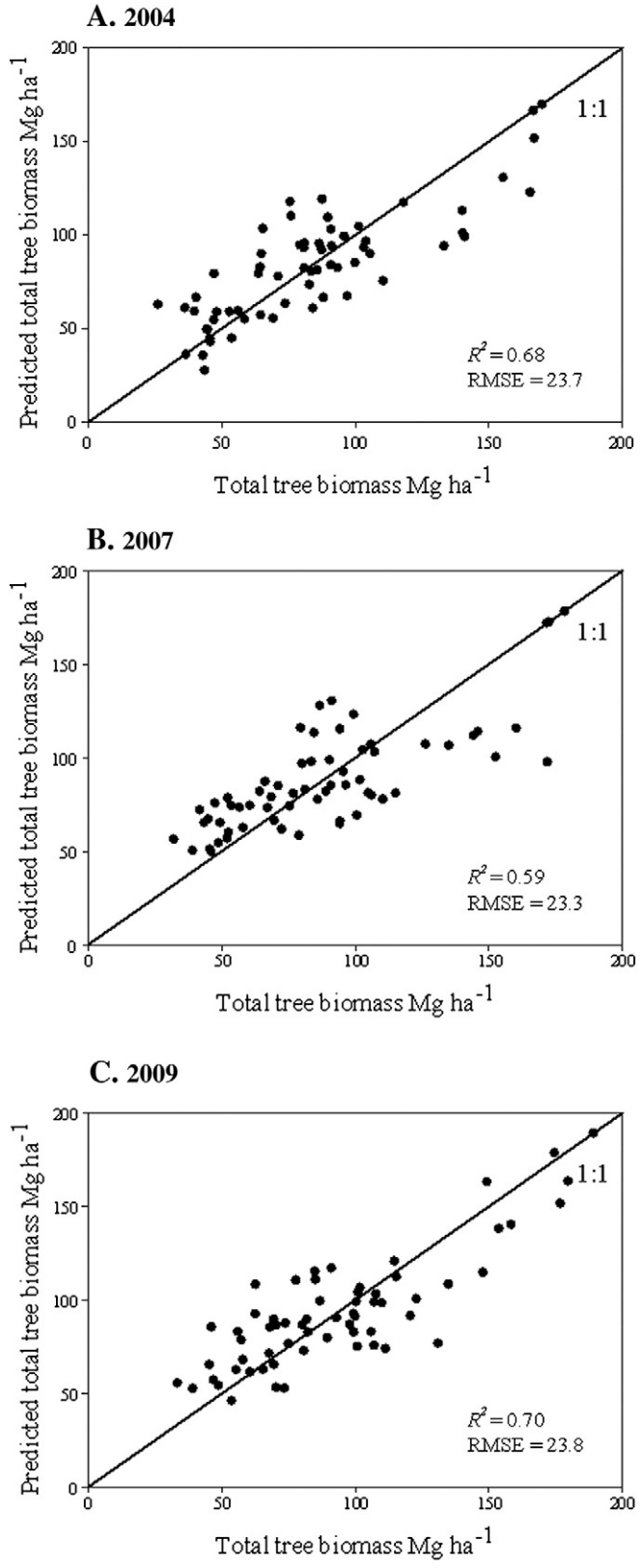

Fig. 2. Model predicted vs. observed total tree biomass for 2004, 2007, and 2009 at 63 field plots.

variability, but with small R^2 values of 0.24, 0.15 and 0.23 for ΔB_{live}, ΔB_{dead}, and ΔB_{total}, respectively (Table 3, Fig. 3A.). Model results for Δ_{07-04} were much stronger, with the prediction of biomass change having nearly the same predictive power as found in the biomass models, with R^2 of 0.66, 0.58, and 0.63 for ΔB_{live}, ΔB_{dead}, and ΔB_{total}, respectively (Table 3, Fig. 3B.). The models predicting biomass change for the full measurement period, Δ_{all}, performed the best, with R^2 values ranging from 0.68 to 0.81 (Table 3, Fig. 3C.). Residual errors were not found to be spatially correlated (Moran's I, $p > 0.05$) for any models. It is also notable that the models for predicting biomass change over the entire period exhibited the least overfit, as indicated by the similar RMSE and $RMSE_{PRESS}$ statistics (Table 3).

Table 3
Statistics for direct estimation of aboveground biomass Δ models developed for Δ_{07-04}, Δ_{09-07}, and Δ_{all} ($n = 63$).

	$n(v)$	$RMSE_{reg}$	$RMSE_{PRESS}$	R^2	Adj. R^2
Δ Live tree biomass (ΔB_{live})					
Δ_{07-04}	9	1.0	1.1	0.24	0.11
Δ_{09-07}	18	6.6	10.0	0.66	0.52
Δ_{all}	18	2.0	3.3	0.81	0.73
Δ Dead tree biomass (ΔB_{dead})					
Δ_{07-04}	5	5.1	7.8	0.16	0.09
Δ_{09-07}	18	12.0	14.6	0.59	0.43
Δ_{all}	13	9.3	12.1	0.72	0.64
Δ Total tree biomass (ΔB_{total})					
Δ_{07-04}	7	1.0	1.1	0.23	0.13
Δ_{09-07}	14	2.1	2.8	0.63	0.53
Δ_{all}	12	1.0	1.3	0.68	0.60

$n(v)$ = number of predictor variables used in the model, $RMSE_{reg}$ = root mean square error of the regression (Mg ha^{-1} yr^{-1}), $RMSE_{PRESS}$ = root mean square error of the PRESS statistic (Mg ha^{-1} yr^{-1}), R^2 = coefficient of determination, Adj. R^2 = adjusted R^2.

4.3.2. Estimation

The direct estimation approach produced means of 2.9 (SE = 0.1), 1.6 (SE = 0.3), and 2.5 (SE = 0.1) Mg ha^{-1} yr^{-1} for change in total tree biomass for Δ_{07-04}, Δ_{09-07}, and Δ_{09-04}, respectively (Table 1). These results illustrate that the direct approach decreased the standard error of the mean biomass change estimate as much as 20 times relative to the indirect approach. The direct estimation approach resulted in smaller variances than the field-based survey for the Δ_{07-04} time period (RE = 1–5.8). It is notable that this time period had little disturbance across the study area and measurements of change were therefore mostly restricted to ecosystem productivity. For the Δ_{09-07} time period, model assisted direct REs were 3.4–5.6, indicating a marked improvement over the efficiency of the field-based estimate. Effectiveness increased further with the model-assisted direct estimation approach when integrated over the full time period Δ_{09-04} (RE = 7.9–10.4).

5. Discussion

The sources of error in ALS-assisted surveys of forest structure and biomass include errors associated with the allometric estimation of field-estimated biomass (e.g. Zhao, Guo, & Kelly, 2012), spatial registration errors in plot location and individual ALS coordinates (e.g. Frazer, Magnussen, Wulder, & Niemann, 2011), and error in the ability of regression models to accurately characterize the plot-level response variables (Skowronski, Clark, Nelson, Hom, & Patterson, 2007). Basal area is typically the strongest predictor of aboveground biomass in many forest types (e.g., Jenkins, Chojnacky, Heath, & Birdsey, 2003), consistent with the allometric models we used to predict oak and pine biomass developed by Whittaker and Woodwell (1968) for Pine Barrens in Long Island, NY. We have previously reported that because the ALS data provides height-based predictor variables of forest structure, biomass predictions based on ALS may not be as accurate in systems where the relationship between stem height and biomass is asymptotic, as is the case for multiple tree species in the study area (Skowronski et al., 2007). Additionally, our study area contained relatively small amounts of aboveground biomass and our training data were mostly homogenous, making it difficult to develop models that did not overfit the field data.

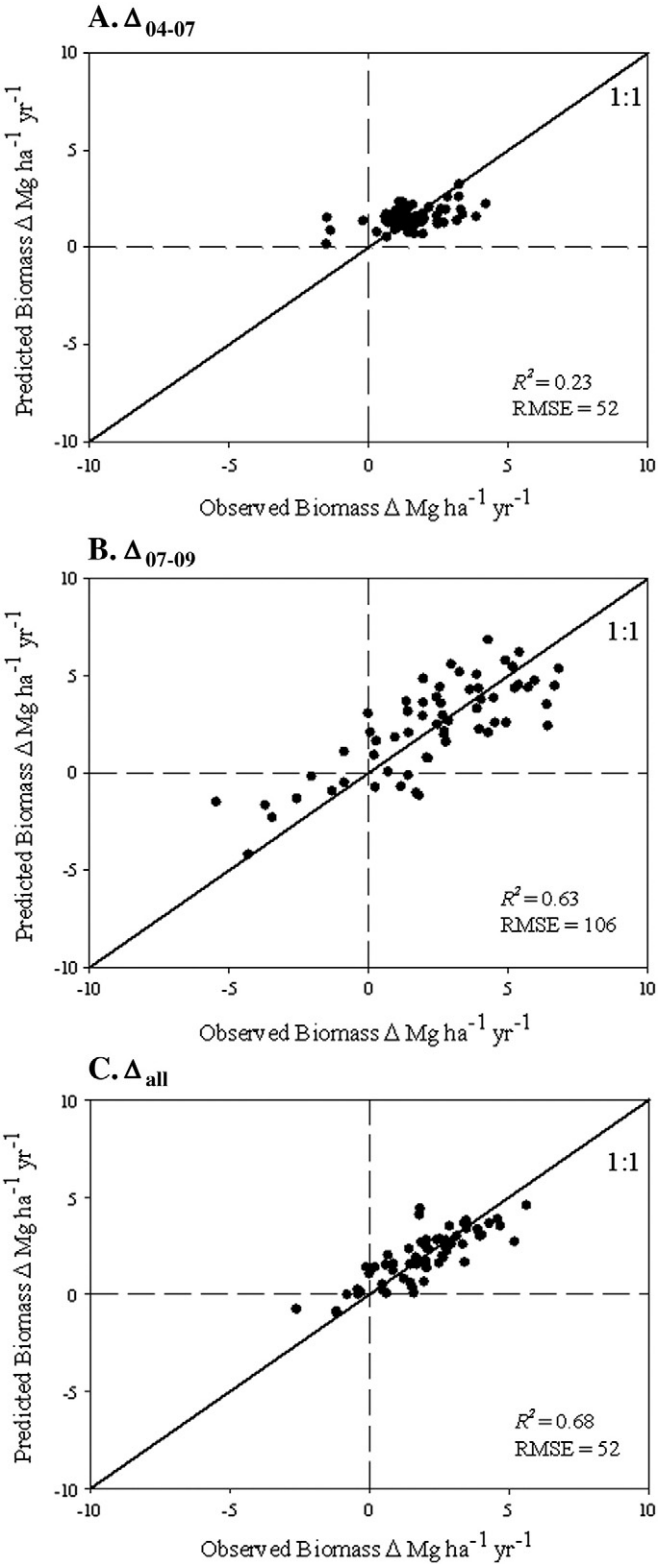

Fig. 3. Predictions of biomass change using the direct prediction method.

However, the accuracies of the B_{total} models presented here (26–29%, RMSE as a % of mean biomass), fall within the range reported in a meta-analysis by Zolkos et al. (2013) for temperate deciduous forests.

Both Mascaro et al. (2011), in a study evaluating sources of uncertainty in ALS-assisted maps of forest carbon, and Næsset et al. (2013), in a study estimating forest biomass change using ALS data, have presented results illustrating how the plot edge effect can negatively impact the estimation biomass in an ALS-assisted survey. The introduction of error by the edge effect can be thought of in the sense of omission or commission. For example, though a stem may fall outside of the physical boundary of a field plot, and therefore not be tallied during the inventory, a proportion of its crown area may still be physically located within the volume of the plot and is sensed by the ALS system. Conversely, a stem may be tallied within the plot while a proportion of the crown is located outside of the plot. As Næsset et al. (2013) and Mascaro et al. (2011) indicated, the edge effect can have less influence on estimation as the edge-to-interior ratio increases with larger plot size and also in more homogeneous forests. The influence of the edge effect in our study is particularly confounding because the heterogeneity of the forest increased over time as a result of the disturbance event. Our estimates of biomass and biomass change were negatively impacted because we used relatively small plots that were not originally intended for our application. Additionally, our plots were likely not the ideal size to best integrate the heterogeneity that resulted from the gypsy moth defoliation.

The calculation of RE allows us to compare the variability of the model-assisted approaches relative to the field-based estimate. The model assisted technique resulted in clear gains in efficiency when estimating biomass components for the three measurement occasions. However, the model assisted estimators produced contrasting results when estimating changes in aboveground biomass. The model assisted-indirect estimation did not improve the uncertainty of the biomass estimates when compared to the field-based SRS estimators. In fact, the resulting variances were an order of magnitude smaller in some cases. These results contrast with an indirect method presented by Hudak et al. (2012), who used sequential ALS acquisitions to predict biomass increment in a commercially harvested, mixed conifer forest in northern Idaho, USA. They reported an overall $R^2 = 0.58$ when differencing predictions from models that were developed from sequential ALS acquisitions (similar to our indirect prediction technique). Their success may be linked to the magnitude of the change that they observed since harvest activities resulted in a mean change of -167 Mg ha^{-1} in disturbed stands. Their model performance was reported to have root mean square deviations (RMSDs) of 92.75 and 101.87 Mg ha^{-1} for T_0 and T_1, respectively (Hudak et al., 2012). In comparison, the disturbance in our study resulted in an average of -8.5 Mg ha^{-1} yr^{-1} being transferred from the live to dead pools, which meant that the RMSE of our B_{total} models (approx. 23 Mg ha^{-1}) is an order of magnitude greater than the change that we attempted to estimate. Thus, the weakness in our results for the indirect prediction approach may be partially due to the discrepancy between the predictive performance of the models of tree biomass and the magnitude of change that was present in the field. Dubayah et al. (2010) had similar conclusions when they attempted to estimate biomass change from LVIS footprints in La Selva, Costa Rica. They had difficulty estimating biomass in older forest types that had little biomass increment, but were more successful in secondary forests with greater growth rates. Because of the magnitude of the prediction errors in the models, and the small biomass increment estimated from the biometric plots across the landscape, this approach may be less suitable for estimating biomass increment at high temporal frequencies or in less productive forests.

In contrast, the model assisted direct estimators had variances that were consistently smaller than the field-based SRS estimators. The REs for these estimators indicate a marked increase in efficiency versus the field-based SRS estimators for both the undisturbed (Δ_{07-04}) and disturbed periods (Δ_{09-07}). The Δ_{09-04} period had the most pronounced increase in efficiency for the model-assisted direct estimation approach. The longer time integration, with greater biomass accumulation for many population elements and substantial shifts in biomass pools from mortality in others, stretched the distributions of both predictor and response variables resulting in the estimation of stronger models. Over this time period, the REs of the biomass change estimation were greater than those of the biomass estimation. These results suggest

that ALS resurvey campaigns could be optimized by estimating expected biomass increments and accounting for the magnitude of the expected change relative to the change in ALS predictor variables.

6. Conclusions

The results of our study illustrate a relative consistency of model error associated with modeling aboveground biomass across ALS collections, evidenced by the similar fit characteristics of models developed for the three separate acquisitions. Our study also echoes the results of Bollandsås et al. (2013) that a direct approach to modeling biomass change with ALS-variables produces models with fit characteristics that are similar to those widely reported (see Zolkos et al., 2013) for single date biomass prediction. We also found that, in our study, a model assisted indirect approach to estimating biomass change did not improve efficiency over field-based SRS estimators. In contrast, a model assisted direct prediction approach produced smaller variances than the SRS estimators. Integrated over the entire time period, these estimators produced REs that indicate even greater gains in efficiency. Future work that takes advantage of an empirical modeling approach could help to determine the temporal thresholds at which sequential ALS acquisitions would provide useful biomass change models under scenarios with varying amounts of change, whether biomass increment or disturbance. The results of our study suggest that these methodologies would perform substantially better when larger changes in aboveground biomass pools were being estimated.

Acknowledgments

This project was funded in part via NASA grant # NNH08AH971 and the National Fire Plan. The authors would like to thank Jason Cole for his help with extracting biometric data from the Tier 3 database. We also thank Matthew Patterson for his work in collecting much of the field data used here. Finally, we thank Ron McRoberts and two anonymous reviewers for their thoughtful comments and suggestions.

References

Andersen, H. E., Strunk, J., Temesgen, H., Atwood, D., & Winterberger, K. (2012). Using multilevel remote sensing and ground data to estimate forest biomass resources in remote regions: A case study in the boreal forests of interior Alaska. *Canadian Journal of Remote Sensing, 37*(6), 596–611.

Asner, G. P., Hughes, R. F., Mascaro, J., Uowolo, A. L., Knapp, D. E., Jacobson, J., et al. (2011). High-resolution carbon mapping on the million-hectare Island of Hawaii. *Frontiers in Ecology and the Environment, 9*, 434–439.

Asner, G. P., Powell, G. V., Mascaro, J., Knapp, D. E., Clark, J. K., Jacobson, J., et al. (2010). High-resolution forest carbon stocks and emissions in the Amazon. *Proceedings of the National Academy of Sciences, 107*(38), 16738–16742.

Blackard, J. A., Finco, M. V., Helmer, E. H., Holden, G. R., Hoppus, M. L., Jacobs, D.M., et al. (2008). Mapping US forest biomass using nationwide forest inventory data and moderate resolution information. *Remote Sensing of Environment, 112*, 1658–1677.

Bollandsås, O. M., Gregoire, T. G., Næsset, E., & Øyen, B. H. (2013). Detection of biomass change in a Norwegian mountain forest area using small footprint airborne laser scanner data. *Statistical Methods & Applications, 1–17*.

Chen, Q. (2007). Airborne LiDAR data processing and information extraction. *Photogrammetric Engineering & Remote Sensing, 73*, 109–112.

Clark, I. A., Phillips, D. R., & Frederick, D. J. (1985). Weight, volume and physical properties of major hardwood species in the Gulf and Atlantic coastal plains. *General technical report SE-250*. Asheville, NC: U.S. Department of Agriculture, Forest Service.

Clark, I. A., Phillips, D. R., & Frederick, D. J. (1986). Weight, volume and physical properties of major hardwood species in the Piedmont. *General technical report SE-255*. Asheville, NC: U.S. Department of Agriculture, Forest Service.

Clark, K. L., Skowronski, N., Gallagher, M., Renninger, H., & Schäfer, K. (2012). Effects of invasive insects and fire on forest energy exchange and evapotranspiration in the New Jersey pinelands. *Agricultural and Forest Meteorology, 166*, 50–61.

Clark, K. L., Skowronski, N. S., & Hom, J. L. (2010). Invasive insects impact forest carbon dynamics. *Global Change Biology, 16*, 88–101.

Dubayah, R. O., Sheldon, S. L., Clark, D. B., Hofton, M.A., Blair, J. B., Hurtt, G. C., et al. (2010). Estimation of tropical forest height and biomass dynamics using LiDAR remote sensing at La Selva, Costa Rica. *Journal of Geophysical Research, 115*.

Ene, L. T., Næsset, E., Gobakken, T., Gregoire, T. G., Ståhl, G., & Holm, S. (2013). A simulation approach for accuracy assessment of two-phase post-stratified estimation in large-area LiDAR biomass surveys. *Remote Sensing of Environment, 133*, 210–224.

Ene, L. T., Næsset, E., Gobakken, T., Gregoire, T. G., Ståhl, G., & Nelson, R. (2012). Assessing the accuracy of regional LiDAR-based biomass estimation using a simulation approach. *Remote Sensing of Environment, 123*, 579–592.

Frazer, G. W., Magnussen, S., Wulder, M.A., & Niemann, K. O. (2011). Simulated impact of sample plot size and co-registration error on the accuracy and uncertainty of LiDAR-derived estimates of forest stand biomass. *Remote Sensing of Environment, 115*, 636–649.

Gobakken, T., Næsset, E., Nelson, R., Bollandsås, O. M., Gregoire, T. G., Ståhl, G., et al. (2012). Estimating biomass in Hedmark County, Norway using national forest inventory field plots and airborne laser scanning. *Remote Sensing of Environment, 123*, 443–456.

Goetz, S. J., Bond-Lamberty, B., Law, B. E., Hicke, J. A., Huang, C., Houghton, R. A., et al. (2012). Observations and assessment of forest carbon dynamics following disturbance in North America. *Journal of Geophysical Research: Biogeosciences (2005–2012), 117*(G2).

Goetz, S., & Dubayah, R. (2011). Advances in remote sensing technology and implications for measuring and monitoring forest carbon stocks and change. *Carbon Management, 2*(3), 231–244.

Gonzalez, P., Asner, G. P., Battles, J. J., Lefsky, M.A., Waring, K. M., & Palace, M. (2010). Forest carbon densities and uncertainties from LiDAR, QuickBird, and field measurements in California. *Remote Sensing of Environment, 114*(7), 1561–1575.

Hocker, H. W., & Early, D. J. (1983). *Biomass and leaf area equations for northern forest species. Research paper, 102*, . Durham, NH: University of New Hampshire Agricultural Experiment Station.

Hollinger, D. Y. (2008). Defining a landscape-scale monitoring tier for the North American carbon program. In C. M. Hoover (Ed.), *Field measurements for forest carbon monitoring* (pp. 3–16). New York, NY: Springer.

Hopkinson, C., Chasmer, L., & Hall, R. J. (2008). The uncertainty in conifer plantation growth prediction from multi-temporal LiDAR datasets. *Remote Sensing of Environment, 112*, 1168–1180.

Houghton, R. A., Hall, F., & Goetz, S. J. (2009). Importance of biomass in the global carbon cycle. *Journal of Geophysical Research: Biogeosciences (2005–2012), 114*(G2).

Hudak, A. T., Strand, E. K., Vierling, L. A., Byrne, J. C., Eitel, J. U. H., Martinuzzi, S., et al. (2012). Quantifying aboveground forest carbon pools and fluxes from repeat LiDAR surveys. *Remote Sensing of Environment, 123*, 25–40.

IPCC (2006). Good practice guidance for land use, land-use change and forestry. http://www.ipcc-nggip.iges.or.jp/public/gpglulucf/gpglulucf.html

Jenkins, J. C., Chojnacky, D. C., Heath, L. S., & Birdsey, R. A. (2003). National-scale biomass estimators for United States tree species. *Forest Science, 49*, 12–35.

Jenkins, J. C., Chojnacky, D. C., Heath, L. S., & Birdsey, R. A. (2004). Comprehensive database of diameter-based biomass regressions for North American tree species. *General technical report NE-319*. Newtown Square, PA: U.S. Department of Agriculture, Forest Service.

Keeley, J. E. (2009). Fire intensity, fire severity and burn severity: A brief review and suggested usage. *International Journal of Wildland Fire, 18*(1), 116–126.

MacArthur, R. H., & Horn, H. S. (1969). Foliage profile by vertical measurements. *Ecology*, 802–804.

Martin, J. G., Kloeppel, B.D., Schaefer, T. L., Kimbler, D. L., & McNulty, S. G. (1998). Aboveground biomass and nitrogen allocation of ten deciduous southern Appalachian tree species. *Canadian Journal of Applied Research, 28*, 1648–1659.

Mascaro, J., Detto, M., Asner, G. P., & Muller-Landau, H. C. (2011). Evaluating uncertainty in mapping forest carbon with airborne LiDAR. *Remote Sensing of Environment, 115*(12), 3770–3774.

Masek, Jeffrey G., et al. (2008). North American forest disturbance mapped from a decadal Landsat record. *Remote Sensing of Environment, 112*(6), 2914–2926.

McRoberts, R. E. (2010). Probability- and model-based approaches to inference for proportion forest using satellite imagery as ancillary data. *Remote Sensing of Environment, 114*, 1017–1025.

McRoberts, R. E., Næsset, E., & Gobakken, T. (2013). Inference for lidar-assisted estimation of forest growing stock volume. *Remote Sensing of Environment, 128*, 268–275.

Myers, R. H. (1990). *Classical and modern regression with applications*. The Duxbury advanced series in statistics and decision science. Boston: PWS-Kent, 171–178.

Næsset, E. (2002). Predicting forest stand characteristics with airborne scanning laser using a practical two-stage procedure and field data. *Remote Sensing of Environment, 80*, 88–99.

Næsset, E., Bollandsås, O. M., Gobakken, T., Gregoire, T. G., & Ståhl, G. (2013). Model-assisted estimation of change in forest biomass over an 11 year period in a sample survey supported by airborne LiDAR: A case study with post-stratification to provide "activity data". *Remote Sensing of Environment, 128*, 299–314.

Næsset, E., & Gobakken, T. (2005). Estimating forest growth using canopy metrics derived from airborne laser scanner data. *Remote Sensing of Environment, 96*(3), 453–465.

Næsset, E., Gobakken, T., Solberg, S., Gregoire, T. G., Nelson, R., Ståhl, G., et al. (2011). Model-assisted regional forest biomass estimation using LiDAR and InSAR as auxiliary data: A case study from a boreal forest area. *Remote Sensing of Environment, 115*(12), 3599–3614.

Pan, Y., Birdsey, R. A., Fang, J., Houghton, R., Kauppi, P. E., Kurz, W. A., et al. (2011). A large and persistent carbon sink in the world's forests. *Science, 333*, 988–993.

Perala, D. A., & Alban, D. H. (1994). Allometric biomass estimators for aspen-dominated ecosystems in the upper Great Lakes. *General technical review NC-314*. St. Paul, MN: U.S. Department of Agriculture, Forest Service.

Särndal, C. -E., Swensson, B., & Wretman, J. (1992). *Model assisted survey sampling*. New York: Springer-Verlag, Inc (694 pp.).

Skowronski, N. S., Clark, K. L., Duveneck, M., & Hom, J. (2011). Three-dimensional canopy fuel loading predicted using upward and downward sensing LiDAR systems. *Remote Sensing of Environment, 115*, 703–714.

Skowronski, N. S., Clark, K. L., Nelson, R., Hom, J., & Patterson, M. (2007). Remotely sensed measurements of forest structure and fuel loads in the Pinelands of New Jersey. *Remote Sensing of Environment*, *108*, 123–129.

Solberg, S., Næsset, E., Hanssen, K. H., & Christiansen, E. (2006). Mapping defoliation during a severe insect attack on Scots pine using airborne laser scanning. *Remote Sensing of Environment*, *102*(3), 364–376.

Vepakomma, U., St-Onge, B., & Keenshaw, D. (2008). Spatially explicit characterization of boreal forest gap dynamics using multi-temporal LiDAR data. *Remote Sensing of Environment*, *112*, 2326–2340.

Vepakomma, U., St-Onge, B., & Keenshaw, D. (2011). Response of a boreal forest to canopy opening: assessing vertical and lateral tree growth with multi-temporal LiDAR data. *Ecological Applications*, *21*, 99–121.

Veraverbeke, S., & Hook, S. J. (2013). Evaluating spectral indices and spectral mixture analysis for assessing fire severity, combustion completeness and carbon emissions. *International Journal of Wildland Fire*, *22*, 707–720.

White, H. (1980). A heteroskedasticity-consistent covariance matrix estimator and a direct test for heteroskedasticity. *Econometrica: Journal of the Econometric Society*, 817–838.

Whittaker, R. H., & Woodwell, G. M. (1968). Dimension and production relations of trees and shrubs in the Brookhaven Forest, New York. *The Journal of Ecology*, *56*, 1–25.

Young, H. E., Ribe, J. H., & Wainwright, K. (1980). Weight tables for tree and shrub species in Maine. *Misc. Report 230*. Orono, ME: University of Maine, Life Sciences and Agriculture Experiment Station.

Yu, X., Hyyppä, J., Kaartinen, H., Hyyppä, H., Maltamo, M., & Rönnholm, P. (2005). Measuring the growth of individual trees using multi-temporal airborne laser scanning point clouds. *Proceedings of the ISPRS Workshop 'Laser Scanning 2005', 12–14 September 2005, Enschede, the Netherlands*, *36*. (pp. 204–208). The Netherlands: GITC bv.

Yu, X., Hyyppä, J., Kaartinen, H., & Maltamo, M. (2004). Automatic detection of harvested trees and determination of forest growth using airborne laser scanning. *Remote Sensing of Environment*, *90*(4), 451–462.

Yu, X., Hyyppä, J., Kaartinen, H., Maltamo, M., & Hyyppä, H. (2008). Obtaining plotwise mean height and volume growth in boreal forests using multi-temporal laser surveys and various change detection techniques. *International Journal of Remote Sensing*, *29*(5), 1367–1386.

Yu, X., Hyyppä, J., Kukko, A., Maltamo, M., & Kaartinen, H. (2006). Change detection techniques for canopy height growth measurements using airborne laser scanner data. *Photogrammetric Engineering and Remote Sensing*, *72*(12), 1339.

Zhao, F., Guo, Q., & Kelly, M. (2012). Allometric equation choice impacts lidar-based forest biomass estimates: A case study from the Sierra National Forest, CA. *Agricultural and Forest Meteorology*, *165*, 64–72.

Zhu, Z., Woodcock, C. E., & Olofsson, P. (2012). Continuous monitoring of forest disturbance using all available Landsat imagery. *Remote Sensing of Environment*, *122*, 75–91.

Zolkos, S. G., Goetz, S. J., & Dubayah, R. (2013). A meta-analysis of terrestrial aboveground biomass estimation using lidar remote sensing. *Remote Sensing of Environment*, *128*, 289–298.